Pathways Towards Habitable Planets
ASP Conference Series, Vol. 430, 2010
Vincent Coudé du Foresto, Dawn M. Gelino, and Ignasi Ribas, eds.

ACCESS: A Concept Study for the Direct Imaging and Spectroscopy of Exoplanetary Systems

J. Trauger,[1] K. Stapelfeldt,[1] W. A. Traub,[1] J. Krist,[1] D. Moody,[1]
E. Serabyn,[1] D. Mawet,[1] L. Pueyo,[1] S. Shaklan,[1] C. Henry,[1] P. Park,[1]
R. Gappinger,[1] P. Brugarolas,[1] J. Alexander,[1] V. Mireles,[1] O. Dawson,[1]
O. Guyon,[2,3] J. Kasdin,[4] B. Vanderbei,[4] D. Spergel,[4] R. Belikov,[5]
G. Marcy,[6] R. Brown,[7] J. Schneider,[8] B. Woodgate,[9] G. Matthews,[10]
R. Egerman,[10] P. Voyer,[10] P. Vallone,[10] J. Elias,[10] Y. Conturie,[10]
R. Polidan,[11] C. Lillie,[11] C. Spittler,[11] D. Lee,[11] R. Hejal,[11]
A. Bronowick,[11]N. Saldivar,[11] M. Ealey,[12] and T. Price[12]

Abstract. ACCESS is one of four medium-class mission concepts selected for study in 2008/9 by NASA's Astrophysics Strategic Mission Concepts Study program. In a nutshell, ACCESS evaluates a space telescope designed for extreme high-contrast imaging and spectroscopy of exoplanetary systems. An actively-corrected coronagraph is used to suppress the glare of diffracted and scattered starlight to the levels required for exoplanet imaging. The ACCESS study asks: What is the most capable medium-class coronagraphic mission that is possible with telescope, instrument, and spacecraft technologies available today?

1. Overview

Our science objective is the direct observation of exoplanetary systems, possibly dynamically full, that harbor exoplanets, planetesimals, and dust/debris structures. Direct coronagraphic imaging at visible (450–900 nm) wavelengths and low-resolution (R=20) spectroscopy of exoplanet systems in reflected starlight

[1]Jet Propulsion Laboratory, Caltech, Pasadena, CA, USA

[2]Subaru Telescope, Hilo, HI, US

[3]University of Arizona, Tucson, AZ, USA

[4]Princeton University, Princeton, NJ, USA

[5]NASA Ames Research Center, Moffett Field, CA, USA

[6]University of California, Berkeley, CA, USA

[7]Space Telescope Science Institute, Baltimore, MD, USA

[8]Paris Observatory, Meudon, France

[9]NASA Goddard Space Flight Center, Greenbelt, MD, USA

[10]ITT Space Systems Division, Rochester, NY, USA

[11]Northrop Grumman Corporation, Redondo Beach, CA, USA

[12]Northrop Grumman Xinetics, Devens, MA, USA

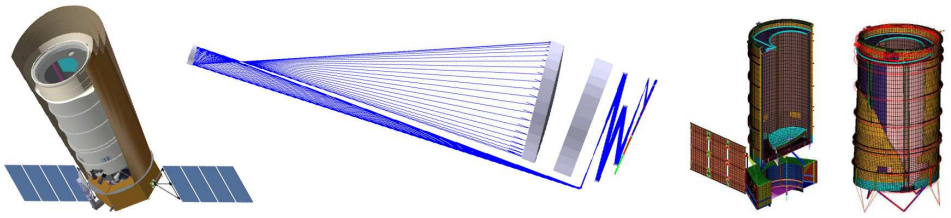

Figure 1. The ACCESS observatory, an actively corrected coronagraphic space telescope for the study of exoplanetary systems.

enables a broad science program that includes a census of nearby known RV planets in orbits beyond ∼1AU; a search for mature exoplanet systems beyond the RV survey limits including giant planets, super-Earths, and possibly a dozen Earth-mass planets; observations of debris structures as indicators of unseen planets and planetesimals; and imaging of dust structures in circumstellar environments as a probe of the life cycle of planetary systems from young stellar objects to proto-planetary nebulae.

The ACCESS study compares the performance and readiness of four major coronagraph architectures. ACCESS defines a conceptual space observatory platform as the "level playing field" for comparisons among coronagraph types. And it uses laboratory validation of four representative coronagraph types as a second "level playing field" for assessing coronagraph hardware readiness. The "external occulter" coronagraph is not considered here, on the presumption that a concept requiring two spacecraft is beyond the bounds of a medium-class mission. ACCESS identifies a genre of scientifically compelling mission concepts built upon mature subsystem technologies, and evaluates science reach of a medium-class coronagraph mission.

2. Performance Assessment

The observatory architecture represents the "best available" for exoplanet coronagraphy within the scope (cost, risk, schedule) of a NASA medium-class mission. Visible wavelengths (450–900 nm) are selected for a minimum inner working angle (IWA). All coronagraphs require an observatory system with exceptional pointing control and optical stability, with deformable mirrors (DMs) for active wavefront control. ACCESS requires systems with high technology readiness (near or above TRL6) for reliable estimates of science capabilities and reliable determinations of cost and schedule. The baseline observatory architecture defines a capable platform for meaningful comparisons among coronagraph types.

The ACCESS observatory (Figure 1) is comprised of a Gregorian telescope with an unobscured 1.5 meter diameter aperture, end-to-end system design for alignment stability, thermal isolation of the telescope secondary mirror and all downstream optics, an precision pointing control system, and an actively-corrected coronagraph for the suppression of diffracted and scattered light. The observatory orbits at L2 halo for a baseline mission of five years.

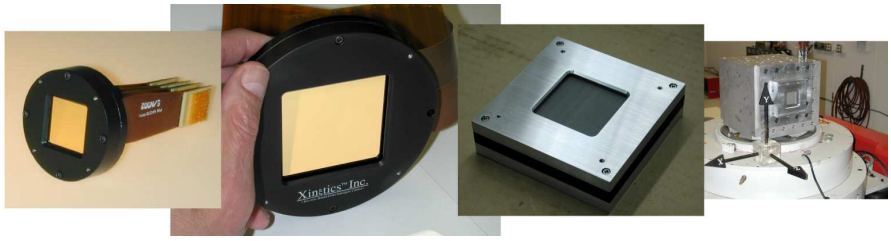

Figure 2. The development of the monolithic PMN deformable mirrors. From left to right: a 32 × 32 mm array (1024 actuators), of the type used for all HCIT demonstrations to date; a 64 × 64 mm array (4096 actuators) first installed on HCIT in 2009; a 48 × 48 mm array (2304 actuators) to be used to demonstrate TRL6 flight-readiness; and the 48 × 48 array on the JPL shake table.

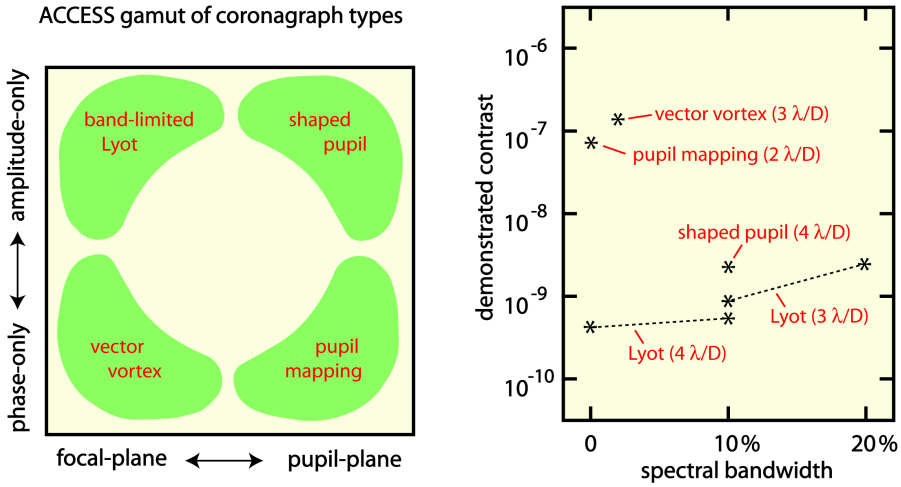

Figure 3. *Left:* The coronograph types in the ACCESS study. *Right:* The best contrast demonstrated in the laboratory to date (September 2009) (see text for details).

High-order wavefront control is provided by a pair of deformable mirrors. The evolution of precision deformable mirrors based on monolithic PMN electroceramic actuator arrays is illustrated in Figure 2. Mirror facesheets are fused silica, with surfaces polished nominally to $\lambda/100$ rms. Surface figure is settable and stable (open loop) to 0.01 nm rms over periods of 6 hours or more in a vacuum testbed environment. All DMs have been manufactured and delivered to JPL by Xinetics Inc.

The gamut of coronagraph types in the ACCESS study is indicated in Figure 3 (at left). The four major coronagraph types perform starlight rejection with combinations of phase and amplitude elements placed in focal and pupil planes.

The best demonstrated laboratory contrast to date (September 2009) for each type is plotted in Figure 3 (at right), as follows. Lyot data at $4\lambda/D$ are TPF performance milestones demonstrated on the High Contrast Imaging Testbed

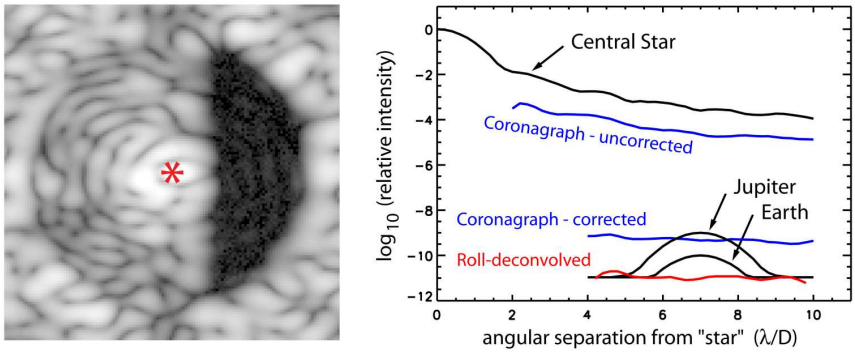

Figure 4. *Left:* The high-contrast dark field (D-shaped) created by a single DM in the laboratory experiments. *Right:* A comparison of the azimuthally averaged PSFs of (a) the star with focal plane mask offset and Lyot stop in place; (b) the coronograph field with all DM actuators set to equal voltages; (c) the coronograph with DM set for a dark half-field and (d) the result of simulated roll deconvolution with the set of 480 consecutive coronograph images. PSFs of a nominal Earth and Jupiter and also indicated (Trauger & Traub 2007).

(HCIT) (Trauger et al. 2006, 2007; Kern et al. 2008) with band limited masks (Kuchner & Traub 2002). Lyot data at $3\lambda/D$ were achieved on the HCIT in the course of the ACCESS study with hybrid Lyot masks (Moody et al. 2008). Shaped pupil (Spergel 2000) data were obtained on the HCIT with masks designed at Princeton (Belikov et al. 2004). Vortex result was demonstrated on the HCIT during the ACCESS study with a vector vortex mask (Mawet et al. 2010). The result for pupil mapping (Guyon et al. 2006) came from the new Ames testbed (Belikov et al. 2009). We note that post-observation data processing methods can be expected to improve the threshold for exoplanet detection by an order of magnitude compared to the raw contrast values plotted in Figure 3, for all coronagraph types, and as illustrated in Figure 4 for the case of a Lyot coronagraph. We further note that significant improvements are expected in the coming months and years as an outcome of active laboratory developments with well-understood technologies.

Coronagraph contrast and stability have been demonstrated in the laboratory at the levels required to detect exoplanets. Figure 4 shows the high-contrast dark field (D-shaped) created by a single DM in laboratory experiments (a pair of DMs clears a full, two-sided dark field). At right in the figure is a comparison of azimuthally averaged PSFs of (a) the star, with focal plane mask offset and Lyot stop in place; (b) the coronagraph field with the DM set to a flat surface figure; (c) the coronagraph with DM set for a dark half-field; and (d) the result of simulated roll deconvolution with the set of 480 consecutive coronagraph images. PSFs of a nominal Earth and Jupiter are also indicated (Trauger & Traub 2007).

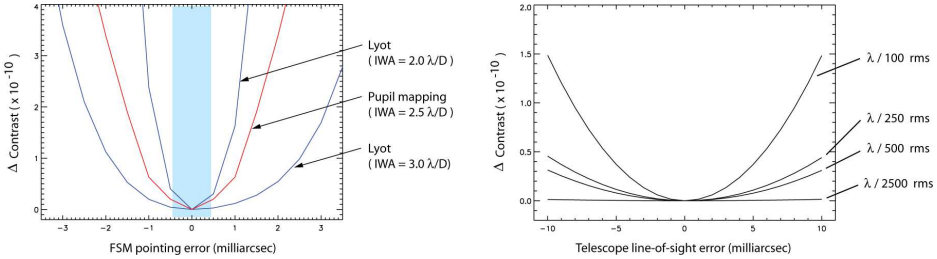

Figure 5. *Left:* Contrast deltas at the IWA for representative coronographs designed for 2.0, 2.5 and 3.0 λ/D. *Right:* Contrast deltas (vs. rms surface figure of the optical elements following the primary mirror) due to beamwalk on the optics upstream of the fine steering mirror.

Structural and thermal models guide the observatory design and inform the optical performance models with estimates of structure dynamics, vibration isolation, pointing control, thermal gradients across the primary mirror and forward metering structures, alignment drift in response to telescope slews and roll.

Telescope body pointing (i.e., line of sight) is stabilized to 1 milliarcsec (3 σ) with an active jitter control system. Figure 5 shows the contrast deltas (vs. rms surface figure of the optical elements following the primary mirror) due to beamwalk on the optics upstream of the fine steering mirror. The telescope attitude control system, augmented by a fine steering mirror within the coronagraph, stabilizes the star image on the coronagraph occulting mask (all four coronagraphs have an occulting mask) to 0.45 milliarcsec (3 σ), as required for high contrast at inner working angles as small as 2 λ/D (Figure 5).

3. Science Program

A baseline minimum science mission has been developed in terms of end-to-end optical models (e.g., Krist 2007) that incorporate the baseline observatory architecture and laboratory-validated estimates of coronagraph performance. A number of results are collected here.

Figure 6 depicts the ACCESS discovery space, which lies above the labeled curve at lower right in the diagram. A 1.5 meter coronagraph in space offers significant contrast advantages over even the largest current and future observatories on the ground.

Figure 7 gives two representations of the completeness in an ACCESS survey for exoplanets. At left are the detections of Jupiter-twins within 45 ° of elongation from their parent stars, to S/N = 10, using the ACCESS Lyot coronagraph with an IWA = 2 λ/D for a number of integration times. Note that the probability that an exoplanet will have a star-planet separation greater than that at 45 ° elongation is 50% or more. At right, the number of planets, in four mass categories, detectable to S/N = 10 in integration times of one day or less, using the ACCESS Lyot coronagraph with an IWA = 2.5 λ/D.

Figure 8 tabulates of the number of nearby stars that could be searched with various ACCESS coronagraphs to the depth of 10-σ detections of Jupiter

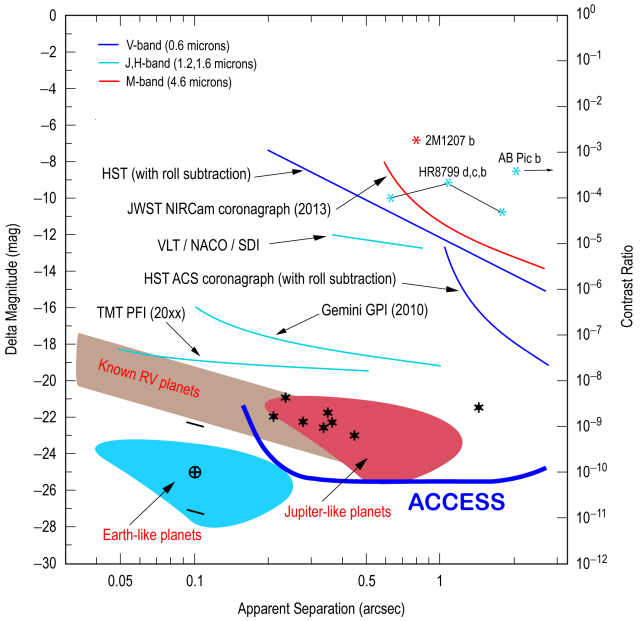

Figure 6. The ACCESS discovery space. Sensitivity for exoplanet detections is compared with current and future observatories in terms of brightness relative to the central star vs. apparent separation. Known exoplanets are shown as asterisks. Shaded areas indicate the regions of high probability of detecting planets orbiting the nearest 100 AFGK stars (for Jupiter-twins in 5AU orbits and Earth-twins in 1 AU orbits, respectively). The detection range for ACCESS is the area above the bold curve at bottom right.

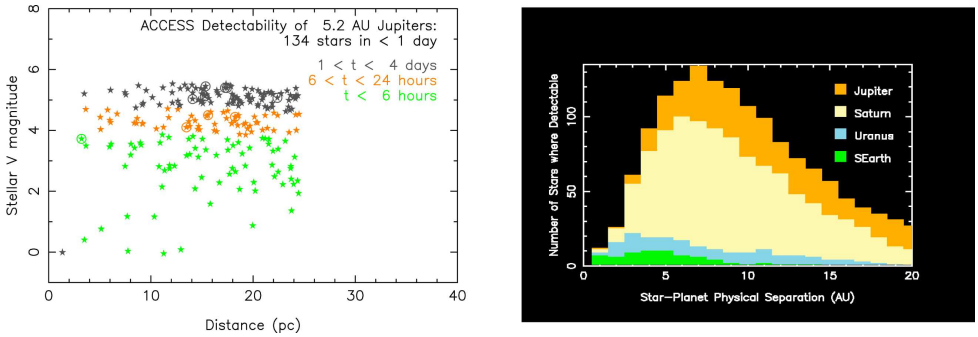

Figure 7. Two representations of the completeness in an ACCESS survey for exoplanets. *Left:* Detections of Jupiter-twins within 45deg of elongation from their parent stars to S/N = 10, using the ACCESS Lyot coronograph with an IWA = 2 λ/D for a number of integration times. *Right:* The number of planets, in four mass categories, detectable to S/N = 10 in integration times of one day or less using the ACCESS Lyot coronograph with an IWAof 2.5 λ/D.

Table 1: Number of nearby stars that can be surveyed for 5.2 AU Jupiters, IWA 3.0 λ/D

Coronagraph Type	Planet 45° from max elong	Planet 15° from max elong
Lyot	117	175
PIAA	166	278
Vortex	135	204

Table 2: Number of nearby stars that can be surveyed for 5.2 AU Jupiters, IWA 2.5 λ/D

Coronagraph Type	Planet 45° from max elong	Planet 15° from max elong
Lyot	153	218
PIAA	178	267
Vortex	154	228

Table 3: Number of nearby stars that can be surveyed for 5.2 AU Jupiters, IWA 2.0 λ/D

Coronagraph Type	Planet 45° from max elong	Planet 15° from max elong
Lyot	170	230
Vortex	164	241

Note: Accurate PIAA wavefront control solution not available for IWA = 2.0 λ/D

Figure 8. The number of nearby stars that could be searched with various ACCESS coronographs to the depth of 10-σ detections of Jupiter-twins in each of six visits to the star over a period of 2.5 years. The arrow corresponds to the ACCESS minimum science program based on current demonstrated technologies. Ongoing developments are expected to bring the demonstrated readiness of other coronagraph configurations to the search sensitivities shown in the table.

twins in each of six visits to the star over a period of 2.5 years. The row indicated by the arrow is an estimate based on coronagraph performance demonstrated in the laboratory at 3.0 λ/D with the Lyot coronagraph. The other rows represent coronagraph performance that may be achieved with further development of known technologies in the near future. The column for 45° from maximum elongation corresponds to an observational completeness of 50% or more in each visit, approaching 100% after six epochs spread over several years.

4. Summary

The ACCESS study has considered the relative merits and readiness of four major coronagraph types, and hybrid combinations, in the context of a conceptual medium class space observatory.

Using demonstrated high-TRL technologies, the ACCESS minimum science program surveys the nearest 120+ AFGK stars for exoplanet systems, and surveys the majority of those for exozodiacal dust to the level of 1 zodi at 3 AU. Discoveries are followed up with R=20 spectrophotometry.

Ongoing technology development and demonstrations in the coming year are expected to further enhance the science reach of an ACCESS mission, in advance of a NASA AO for a medium class mission. The study also identifies areas of technology development that would advance the readiness of all major coronagraph types in the coming 5 years.

Acknowledgments. The research described in this paper was carried out at the Jet Propulsion Laboratory, California Institute of Technology, under a contract with the National Aeronautics and Space Administration.

References

Belikov, R., et al. 2009, in Techniques and Instrumentation for Detection of Exoplanets IV, ed. Shaklan, S. B., SPIE, 7440, 74400J
Belikov, R., Kasdin, N.J., & Vanderbei, R.J. 2006, ApJ, 652, 833
Giveón, A., et al. 2007, in Astronomical Adaptive Optics Systems and Applications III, ed. Tyson, R. K. & Lloyd-Hart, M., SPIE, 6691, 66910A
Guyon, O., et al. 2005, ApJ, 622, 744
Guyon, O., et al. 2008, in Space Telescopes and Instrumentation 2008: Optical, Infrared, and Millimeter, ed. Oschmann, et al., SPIE, 7010, 70102Z
Kern, B., et al. 2008, JPL Document D-60951
Krist, J.E. 2007, in Optical Modeling and Performance Predictions III, ed. Kahan, M. A., SPIE, 6675, 66750P
Kuchner, M.J., & Traub, W.A. 2002, ApJ, 570, 900
Mawet, D., et al. 2010, ApJ, 709, 53
Moody, D., Gordon, B., & Trauger, J. 2008, in Space Telescopes and Instrumentation 2008: Optical, Infrared, and Millimeter, ed. Oschmann, et al., SPIE, 7010, 701081
Spergel, D.N. 2000, arXiv:astro-ph/0101142v1
Trauger, J., et al. 2006, JPL Document D-35484
Trauger, J., et al. 2007, SPIE, 6693, 66930X
Trauger, J.T., & Traub, W.A. 2007, Nat, 446, 771
Trauger, J., et al. 2009, ACCESS final report to NASA (copies available on request)